NANO LETTERS

Letter

pubs.acs.org/NanoLett

Colloidal $CdSe_{1-x}S_x$ Nanoplatelets with Narrow and Continuously-Tunable Electroluminescence

Fengjia Fan,[†] Pongsakorn Kanjanaboos,[†] Mayuran Saravanapavanantham,[†] Eric Beauregard,[†] Grayson Ingram,[‡] Emre Yassitepe,[†] Michael M. Adachi,[†] Oleksandr Voznyy,[†] Andrew K. Johnston,[†] Grant Walters,[†] Gi-Hwan Kim,[†] Zheng-Hong Lu,[‡] and Edward H. Sargent*[,†]

[†]Department of Electrical and Computer Engineering and [‡]Department of Materials Science and Engineering, University of Toronto, 10 King's College Road, Toronto, Ontario M5S 3G4, Canada

Supporting Information

ABSTRACT: Colloidal nanoplatelets, quasi-two-dimensional quantum wells, have recently been introduced as colloidal semiconductor materials with the narrowest known photoluminescence line width (~10 nm). Unfortunately, these materials have not been shown to have continuously tunable emission but rather emit at discrete wavelengths that depend strictly on atomic-layer thickness. Herein, we report a new synthesis approach that overcomes this issue: by alloying CdSe colloidal nanoplatelets with CdS, we finely tune the emission spectrum while still leveraging atomic-scale thickness control. We proceed to demonstrate light-emitting diodes with sub-bandgap turn-on voltages (2.1 V for a device emitting at 2.4 eV) and the narrowest electroluminescence spectrum (FWHM ~12.5 nm) reported for colloidal semiconductor LEDs.

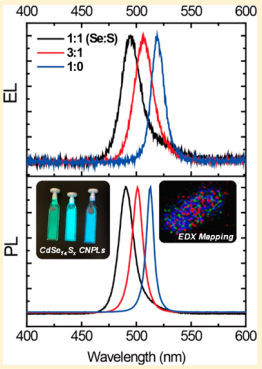

KEYWORDS: *$CdSe_{1-x}S_x$, colloidal nanoplatelets, solution-processed light-emitting diodes, alloying, electroluminescence*

In light emission, colloidal quantum confined nanostructures have drawn considerable attention due to their high emission efficiency and quantum-tuned emission spectra.[1−5] Over the past two decades, syntheses of colloidal quantum dots (CQDs) have been developed that cover continuously the ultraviolet (UV), visible (vis), and near-infrared (NIR).[4] With quantum confinement in all three dimensions, CQDs exhibit a bandgap that can be finely tuned by adjusting nanoparticle size; however, they also suffer from inhomogeneous broadening[6] introduced by uncontrolled size variations in all three dimensions.

In the past few years, great strides have been made in the synthesis of colloidal nanoplatelets (CNPLs). CNPLs show confinement along one axis and can exhibit extremely narrow emission line widths on the order of 10 nm.[7−10] Through careful synthesis, one can achieve atomically flat CNPLs and therefore monolayer (ML) thickness control.[8] This leads to narrow emission resulting from minimal inhomogeneous broadening.[11]

Sharp luminescence makes CNPLs promising for precise-color displays and as high-density optical gain media.[12,13] In particular, CNPLs can potentially be applied as light sources for 3D laser projection where small FWHMs are necessary.[14] However, CNPLs fail to provide continuous spectral tunability. To illustrate, varying the number of monolayers in CdSe CNPLs produces discrete emission wavelengths peaking at 460, 510, or 550 nm using 5, 6, or 7 ML.[9] There have been efforts to adjust the bandgap of the CNPLs finely through compositional control; however, continuously tunable PL in CNPLs still has yet to be shown.[15,16]

Herein, we retain CNPL emission sharpness, and add continuous tunability. We do so by alloying while maintaining fixed monolayer thickness. In this study, we demonstrate emission covering the green to blue transition regime (513−481 nm) via CdS-alloying of 6 ML CdSe CNPLs.

In synthesis, we introduce CdS components to the CdSe CNPLs by using mixtures of elemental Se and S powders in different molar ratios as the anion sources (see Supporting Information for synthesis details). We focused on 6 ML thick CdSe CNPLs because they emit at 510 nm, while 5 ML CdSe CNPLs emit at 460 nm. Filling this gap completes a spectral range in which the human eye is very color-sensitive.

Previous studies have demonstrated precise thickness and shape (cubic/rectangular) control in CdSe CNPLs.[8,9] In contrast, CdS CNPLs generally lack thickness or shape control.[9,10] We started the synthesis of alloyed CNPLs from a low S fraction and found that when we used a 3:1 ratio of Se to S, we obtain CNPLs with regular dimensions similar to those of pure CdSe CNPLs. When we further decrease the Se/S ratio to 1:1, transmission electron microscope (TEM) imaging revealed mostly CQDs rather than CNPLs.

Received: March 30, 2015
Revised: May 26, 2015

DOI: 10.1021/acs.nanolett.5b01233
Nano Lett. XXXX, XXX, XXX−XXX

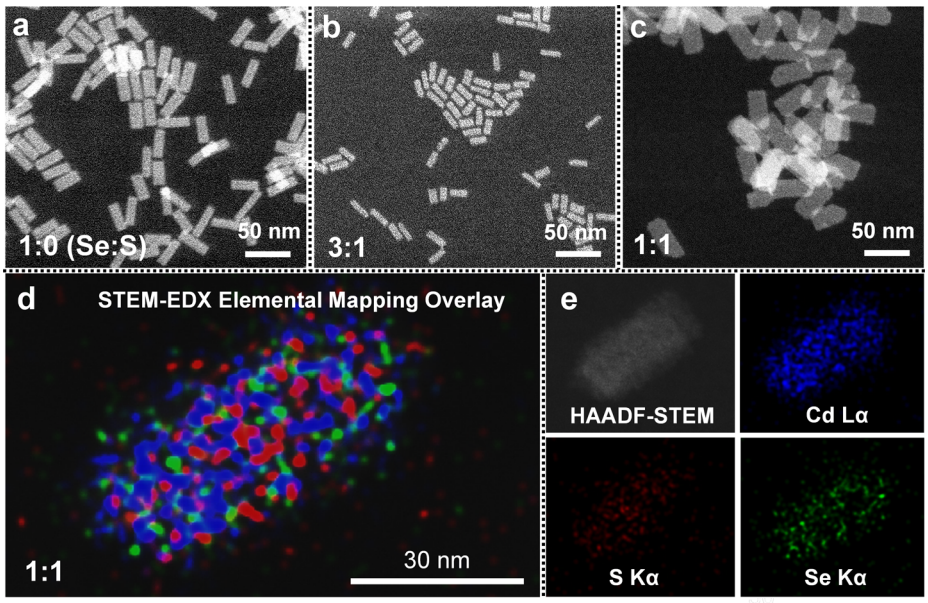

Figure 1. HAADF-STEM and STEM-EDX elemental mapping images of $CdSe_{1-x}S_x$ CNPLs. (a–c) HAADF-STEM images of CNPLs with Se/S ratio of 1:0, 3:1, and 1:1, respectively. Large atomic number differences between the CNPLs and the carbon support on TEM grids generate high contrast in HAADF-STEM images that clearly show the regular and rectangular shaped thin CNPLs. (d,e) High-resolution STEM-EDX elemental mapping of CNPLs with 1:1 Se/S ratio. Cd (blue), Se (green), and S (red) components are shown to be evenly distributed in the single CNPL.

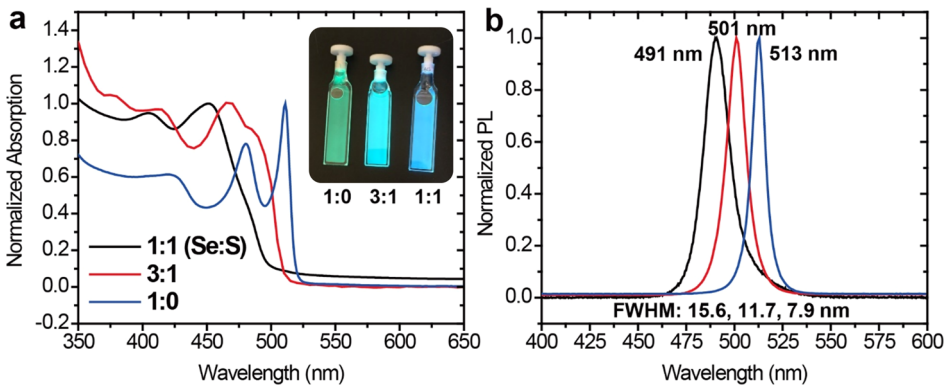

Figure 2. Optical properties of CNPLs. (a) UV–vis absorption and (b) PL spectra of 1:0, 3:1, and 1:1 $CdSe_{1-x}S_x$ CNPLs. Both the absorption peaks from light/heavy-hole transitions and band-edge PL peaks shift to higher energies with increasing S fractions, indicating the widening bandgap. The continuous evolution of absorption and PL peaks confirms that the thickness of the CNPLs remain unchanged. The inset is a photograph of the CNPLs emitting under the UV lamp (~355 nm).

When we used previously reported CNPLs syntheses,[17] we found that there existed CQDs as a byproduct of the reaction. These could be easily separated from the CNPLs due to their better dispersibility in nonpolar solvents such as hexane. Smaller size and weaker vander Waals forces between CQDs explain this characteristic. However, CNPLs also show very good colloidal stability at low concentrations. They can therefore be selectively precipitated only when the CNPLs are the dominant product of the reaction.

Consequently, we sought to develop a simple protocol to synthesize $CdSe_{1-x}S_x$ CNPLs with high yields at high S fractions. We were able to achieve this with the use of larger quantities of the precursors and with hexane injections. We propose that these nonpolar solvent injections better stabilize the CQDs in the supernatant and prevent their precipitation during the washing process.

Powder X-ray diffraction (PXRD) measurements were carried out to characterize the crystalline structure of the alloyed CNPLs. As shown in Supporting Information Figure S1, the synthesized CNPLs were confirmed to crystallize in a zincblende structure and the lattice constant gradually decreases with decreasing the Se/S ratio. Moreover, no diffraction peak splitting was observed, confirming the formation of $CdSe_{1-x}S_x$ alloys. The actual Se/S ratios in the $CdSe_{1-x}S_x$ CNPLs, characterized by X-ray photoelectron spectroscopy (XPS), differ slightly from the Se/S ratios used in synthesis (see Supporting Information Table S1). We observe that the sulfur component of the alloyed CNPLs exceeds the proportion in which it was included in the precursors; for example, 3:1 precursor ratio (Se/S) yielded CNPLs with 66% Se and 34% S. Hereafter, we identify different CNPLs using the Se/S precursor ratio used for their respective syntheses (e.g., 1:1). Because CNPLs show very low contrast in bright-field transmission electron microscope (BF-TEM) images, high-angle annular dark-field scanning transmission electron microscopy (HAADF-STEM) was used for imaging

DOI: 10.1021/acs.nanolett.5b01233
Nano Lett. XXXX, XXX, XXX–XXX

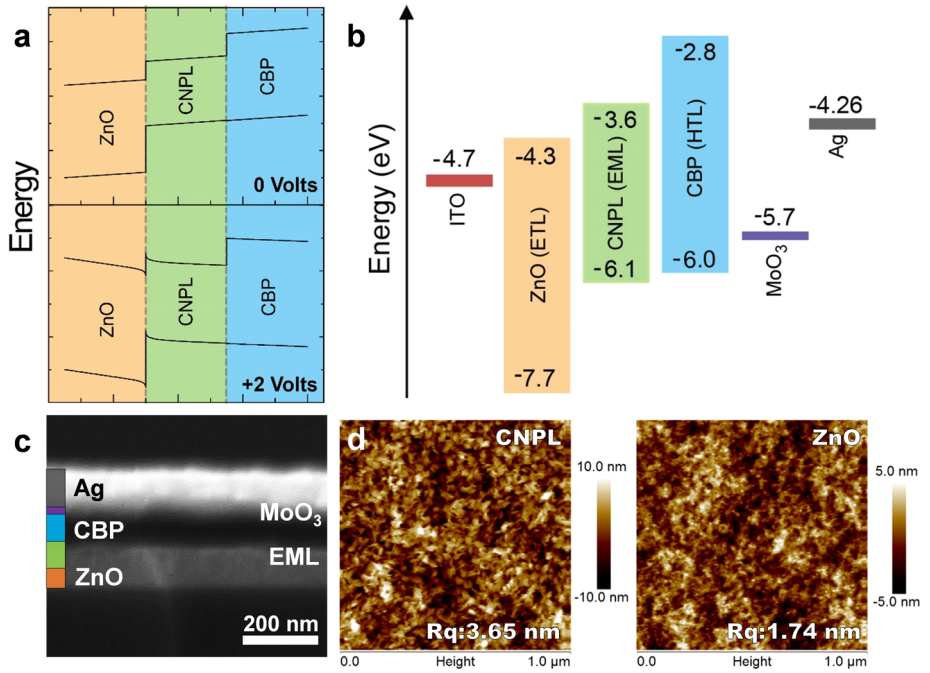

Figure 3. CNPLs LED device architecture characterization. (a) Device under zero-bias and forward bias near turn-on voltage (2 V), modeled using SCAPS. (b) Band diagram of the device. (c) Cross-sectional SEM imaging reveals different layers in the device and their respective thicknesses. (d) AFM measurements allow characterization of roughness of the solution-processed layers. The measurement on the left is of the EML spin-coated on top of the ETL (surface roughness Rq = 3.56 nm), whereas the measurement on the right is of the ETL only (surface roughness Rq = 1.74 nm).

(Figure 1a–c). Our $CdSe_{1-x}S_x$ CNPLs (1:0, 3:1, and 1:1) show uniform morphology with typical lengths of 34 ± 4, 20 ± 4, and 48 ± 3 nm and widths of 12 ± 2, 8 ± 1, and 20 ± 2 nm, respectively. The homogeneity of S and Se distributions in CNPLs was confirmed by scanning transmission electron microscope–energy dispersive X-ray spectroscopy (STEM-EDX) elemental mapping (Figure 1d, e).

The optical properties of the CNPLs were characterized via UV–vis absorbance and photoluminescence (PL) spectroscopy (Figure 2). The bandgaps of alloyed CNPLs increase with increasing S fractions. The first two exciton peaks from pure CdSe CNPLs are related to light-hole and heavy-hole transitions, and the splitting energy depends on the atomic mass.[9] With increasing S content, the absorption peaks associated with the two transitions in 1:0 CNPLs tend to merge into a single peak. Notably, the widths of the absorption peaks become broader after alloying with CdS, indicating that some amount of composition variation may occur within CNPLs or among different CNPLs. The PL peaks continuously blue shift from 513 to 501 nm, and 491 nm, which span the emission gap of the 5 and 6 ML CdSe CNPLs. The corresponding full width half-maximum (FWHM) of the PL spectra are 8, 12, and 16 nm, respectively. The photoluminescence quantum yield decreases from 37 to 23% and to 10% in 1:0, 3:1, and 1:1 solution samples, respectively. This indicates that the dangling bonds from the CdS component are less well-passivated than those from the CdSe component. Additionally, we show the optical characteristics of alloyed CNPLs emitting at 481 nm (Supporting Information Figure S2). The human eye is very sensitive to color change in this regime, and thanks to the narrow emission bandwidth even a change of 10 nm in emission wavelength can be clearly observed (inset photograph in Figure 2a). As a result, the color gamut in LCD displays can be significantly improved when green emitters with narrow bandwidth are used.[18]

We proceeded to fabricate electroluminescent devices employing $CdSe_{1-x}S_x$ CNPLs. A thin layer of CNPLs is stacked between organic and inorganic charge transport layers (CTLs) to form a structure similar to the hybrid architectures employed in CQD-LEDs.[3−5,19−22] An inverted device structure with such CTLs was chosen as it has shown promise in both brightness and record efficiencies for CQD-LEDs[3,4,22,23] while enabling systematic engineering of CTLs in the device fabrication process without degrading the CNPL layers. The optimized structure is shown in Figure 3b, where solution-processed ZnO functions as the electron transport layer (ETL) while 4,4′-bis(*N*-carbazolyl)-1,1′-biphenyl (CBP) acts as the hole transport layer (HTL). ZnO is known to transport and inject electrons[22,23] efficiently into the emissive layer (EML).

To prevent electron–hole imbalance, a careful choice of HTL is necessary to facilitate hole transport. To facilitate selection of a suitable HTL candidate, UPS was carried out on 1:0 platelets (Supporting Information Figure S3) and the conduction and valence bands were measured as −3.62 and −6.05 eV, respectively. CBP with its deep HOMO at −6 eV is well-aligned with the valence band of the platelets. Figure 3a shows the energy band diagram of the device under zero-bias and 2 V forward-bias according to the SCAPS[24] simulator. When we included the hole-injecting layer (HIL) MoO_3, the best performance was achieved. Other HILs screened included 4,4′-cyclohexylidenebis[*N*,*N*-bis(4-methylphenyl)-benzenamine] (TAPC) and *N*,*N*′-di(1-naphthyl)-*N*,*N*′-diphenyl-(1,1′-biphenyl)-4,4′-diamine (NPB). By using the inverted structure, we were able to carry out sequential high-vacuum thermal vapor deposition of CBP, MoO_3, and the metal contacts in a continuous manner, without having to interrupt the procedure to deposit solution-processed layers in between.

DOI: 10.1021/acs.nanolett.5b01233
Nano Lett. XXXX, XXX, XXX–XXX

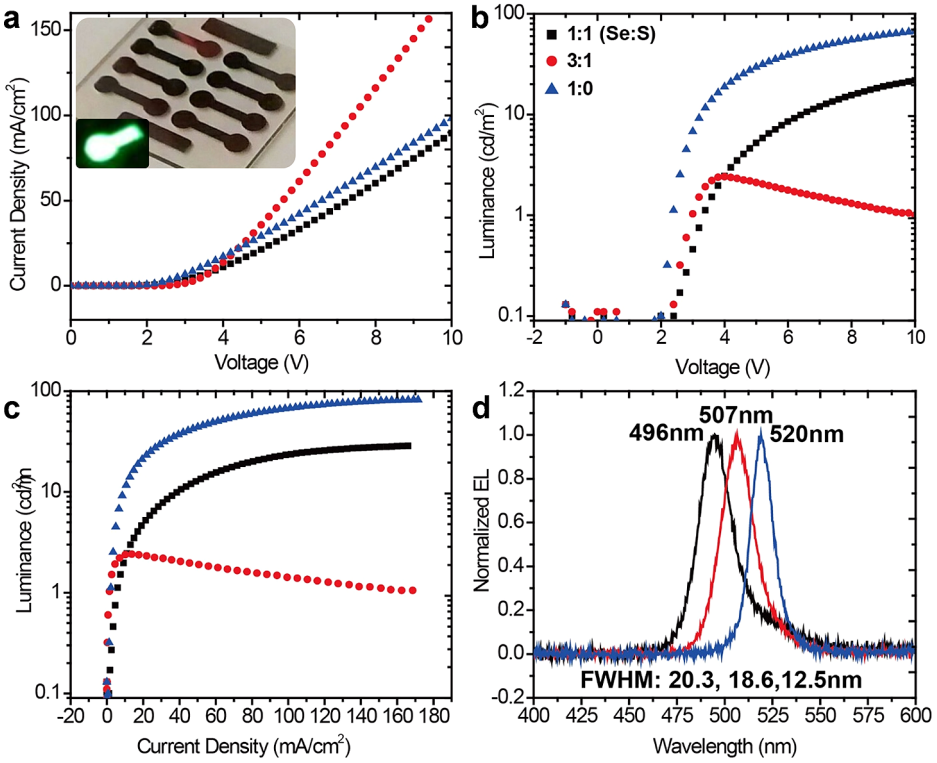

Figure 4. CNPLs LED device performance characteristics. (a) Current density−voltage, (b) luminance−voltage, (c) luminance−current density, (d) EL spectrum of 1:0 CNPL (blue), 3:1 CNPL (red), and 1:1 CNPL (black). Photograph of device and its electroluminescence (a, inset) is shown. Turn-on voltage of the devices were 2.1, 2.2, and 2.4 V for the 1:0, 3:1, and 1:1 CNPLs devices, respectively (showing sub-bandgap turn-on).

Cross-sectional SEM imaging of a device, Figure 3c, reveals the thicknesses of different layers: 50 nm ZnO, 70 nm EML, 65 nm CBP, 10 nm MoO_3, and a 100 nm metal contact (Ag or Al). The thickness of the EML was measured independently using atomic force microscopy (AFM) scratch test measurement (Supporting Information Figure S4). The ZnO solution was synthesized by a method previously reported.[23] We found that other ZnO methods, that is, sputtering, atomic layer deposition (ALD), and ZnO nanoparticles,[25] used in record CQD solar cells do not offer similarly good LED performance. We posit that slight shifts in band alignment and surface morphology could affect electron injection efficiency and thus degrade these other routes.

ZnO films were deposited via spin-coating onto a patterned ITO/glass substrate at 2000 rpm for 30 s and baked at 350 °C for 10 min. Subsequently, the CNPLs were spin-coated onto the ZnO films at 1500 rpm for 20 s. AFM measurements indicate surface roughness (Rq) of less than 5 nm (Figure 3d and Supporting Information Figure S5).

Both ZnO and thermally evaporated CBP do not significantly quench the emission from the adjacent nanoplatelets layer. The average PLQY of the pure CdSe CNPL films on ZnO/ITO is 3−5%. Solution-processed CBP, and more generally, the use of any other polar solvents, greatly reduced the photoluminescence of the CNPL films, and it is for this reason that we avoided it. Fabricated devices were stored in a glovebox and tested in a nitrogen environment. Devices were coated with SiO to reduce humidity damage when tested in air.

Figure 4 shows the electroluminescence characteristics: current density−voltage, EL spectra, luminance−voltage, and current efficiencies for devices from pure and alloyed CNPLs. Because of efficient direct exciton recombination from the inverted structure[22,23] our devices (see Figure 4b) have sub-bandgap turn on voltages (<2.5 V) with luminance on the order of 10−100 Cd/m^2. The 3:1 CNPL devices were more sensitive to high current and started to degrade at high current density (~10 mA/cm^2). We observed no parasitic emission from any of the other layers over the voltage range of our measurement.

As in previously reported CNPL LEDs,[26,27] current efficiencies remain low compared to CQD LEDs.[3,22] From PL lifetime measurements (Supporting Information Figure S6) comparing both CNPLs on ZnO and CNPLs on glass, the lifetimes do not vary greatly. Thus, the loss mechanism is not caused by nonradiative energy transfer to the ETL. Ultrafast picosecond energy transfer between CNPLs,[28] leading to low film PLQYs, is believed to be the dominant cause.

This work illustrates the narrowest tunable EL spectra reported for colloidal semiconductor LEDs.[26,27] The slight broadening and red shifting of EL relative to the PL spectra is associated with optical phonon coupling and quantum confined stark effects previously shown in CQD and CNPL EL devices.[26,29,30]

Through this Letter, we report a new synthesis approach to introduce CdS components into CdSe CNPLs of fixed thickness, thereby bridging the emission gap between CNPLs of different thicknesses. Deploying low-cost, solution-processed materials with an inverted LED design, for the first time we demonstrate tunable LEDs with low turn on voltages and the purest color emission reported for colloidal materials.

■ ASSOCIATED CONTENT

Supporting Information

PXRD and XPS measurements of reported CNPLs, HAADF-STEM image and absorption/PL spectra of 481 nm emitting

DOI: 10.1021/acs.nanolett.5b01233
Nano Lett. XXXX, XXX, XXX−XXX

CNPLs, UPS measurement of 1:0 CNPLs, PL decay measurements, EML thickness and roughness over large scales, CNPL synthesis protocols, and materials characterization methods. The Supporting Information is available free of charge on the ACS Publications website at DOI: 10.1021/acs.nanolett.5b01233.

AUTHOR INFORMATION

Corresponding Author

*E-mail: ted.sargent@utoronto.ca.

Author Contributions

F.F., P.K., and M.S. contributed equally.

Notes

The authors declare no competing financial interest.

ACKNOWLEDGMENTS

This publication is based in part on work supported by Award KUS-11-009-21, made by King Abdullah University of Science and Technology (KAUST), by the Ontario Research Fund - Research Excellence Program, and by the Natural Sciences and Engineering Research Council (NSERC) of Canada. E.Y. acknowledges support from FAPESP-BEPE (2014/18327-9) fellowship. The authors thank S. Hoogland, D. Sellan, X. Lan, Z. Yang, and L. Quan for useful discussions. The authors thank L. Levina, E. Palmiano, R. Wolowiec, and D. Kopilovic for their technical help over the course of this study. We thank the Centre for Microfluidic Systems in Chemistry and Biology (Toronto, Ontario) for access to the atomic force microscope.

REFERENCES

(1) Colvin, V. L.; Schlamp, M. C.; Alivisatos, A. P. Light-Emitting-Diodes Made from Cadmium Selenide Nanocrystals and a Semiconducting Polymer. *Nature* **1994**, *370*, 354−357.

(2) Sun, L.; et al. Bright infrared quantum-dot light-emitting diodes through inter-dot spacing control. *Nat. Nanotechnol.* **2012**, *7*, 369−373.

(3) Mashford, B. S.; et al. High-efficiency quantum-dot light-emitting devices with enhanced charge injection. *Nat. Photonics* **2013**, *7*, 407−412.

(4) Shirasaki, Y.; Supran, G. J.; Bawendi, M. G.; Bulović, V. Emergence of colloidal quantum-dot light-emitting technologies. *Nat. Photonics* **2013**, *7*, 13−23.

(5) Dai, X.; et al. Solution-processed, high-performance light-emitting diodes based on quantum dots. *Nature* **2014**, *515*, 96−99.

(6) Empedocles, S. a; Neuhauser, R.; Shimizu, K.; Bawendi, M. G. Photoluminescence from single semiconductor nanostructures. *Adv. Mater.* **1999**, *11*, 1243−1256.

(7) Joo, J.; Son, J. S.; Kwon, S. G.; Yu, J. H.; Hyeon, T. Low-Temperature Solution-Phase Synthesis of Quantum Well Structured CdSe Nanoribbons. *J. Am. Chem. Soc.* **2006**, *128*, 5632−5633.

(8) Ithurria, S.; Dubertret, B. Quasi 2D Colloidal CdSe Platelets with Thicknesses Controlled at the Atomic Level. *J. Am. Chem. Soc.* **2008**, *130*, 16504−16505.

(9) Ithurria, S.; et al. Colloidal nanoplatelets with two-dimensional electronic structure. *Nat. Mater.* **2011**, *10*, 936−941.

(10) Li, Z.; et al. Uniform thickness and colloidal-stable CdS quantum disks with tunable thickness: Synthesis and properties. *Nano Res.* **2012**, *5*, 337−351.

(11) Tessier, M. D.; Javaux, C.; Maksimovic, I.; Loriette, V.; Dubertret, B. Spectroscopy of Single CdSe Nanocrystallites. *ACS Nano* **2012**, *6*, 6751−6758.

(12) She, C.; Fedin, I.; Dolzhnikov, D. Low-threshold stimulated emission using colloidal quantum wells. *Nano Lett.* **2013**, *14*, 2772−2777.

(13) Grim, J. Q.; et al. Continuous-wave biexciton lasing at room temperature using solution-processed quantum wells. *Nat. Nanotechnol.* **2014**, *9*, 891−895.

(14) Geng, J. Three-dimensional display technologies. *Adv. Opt. Photonics* **2013**, *5*, 456−535.

(15) Sokolikova, M. S.; Shlenskaya, N. N.; Kozlovskii, V. F.; Vasiliev, R. B.; Gaskov, a. M. Synthesis and optical properties of quasi-2D CdS_xSe_{1-x} nanoparticles. *Russ. J. Inorg. Chem.* **2014**, *59*, 1069−1072.

(16) Maiti, P. S.; Meir, N.; Houben, L.; Bar-Sadan, M. Solution phase synthesis of homogeneously alloyed ultrathin CdS_xSe_{1-x} nanosheets. *RSC Adv.* **2014**, *4*, 49842−49845.

(17) Mahler, B.; Nadal, B.; Bouet, C.; Patriarche, G.; Dubertret, B. Core/Shell Colloidal Semiconductor Nanoplatelets. *J. Am. Chem. Soc.* **2012**, *134*, 18591−18598.

(18) Pust, P.; Schmidt, P. J.; Schnick, W. A revolution in lighting. *Nat. Mater.* **2015**, *14*, 454−458.

(19) Anikeeva, P. O.; Halpert, J. E.; Bawendi, M. G.; Bulović, V. Quantum Dot Light-Emitting Devices with Electroluminescence Tunable over the Entire Visible Spectrum. *Nano Lett.* **2009**, *9*, 2532−2536.

(20) Caruge, J. M.; Halpert, J. E.; Wood, V.; Bulović, V.; Bawendi, M. G. Colloidal quantum-dot light-emitting diodes with metal-oxide charge transport layers. *Nat. Photonics* **2008**, *2*, 247−250.

(21) Qian, L.; Zheng, Y.; Xue, J.; Holloway, P. H. Stable and efficient quantum-dot light-emitting diodes based on solution-processed multilayer structures. *Nat. Photonics* **2011**, *5*, 543−548.

(22) Kwak, J.; et al. Bright and Efficient Full-Color Colloidal Quantum Dot Light-Emitting Diodes Using an Inverted Device Structure. *Nano Lett.* **2012**, *12*, 2362−2366.

(23) Supran, G. J.; et al. High-Performance Shortwave-Infrared Light-Emitting Devices Using Core−Shell (PbS−CdS) Colloidal Quantum Dots. *Adv. Mater.* **2015**, *27*, 1437−1442.

(24) Burgelman, M.; Nollet, P.; Degrave, S. Modelling polycrystalline semiconductor solar cells. *Thin Solid Films* **2000**, *361*, 527−532.

(25) Chuang, C.-H. M.; Brown, P. R.; Bulović, V.; Bawendi, M. G. Improved performance and stability in quantum dot solar cells through band alignment engineering. *Nat. Mater.* **2014**, *13*, 1−6.

(26) Chen, Z.; Nadal, B.; Mahler, B.; Aubin, H.; Dubertret, B. Quasi-2D colloidal semiconductor nanoplatelets for narrow electroluminescence. *Adv. Funct. Mater.* **2014**, *24*, 295−302.

(27) Vitukhnovsky, a. G.; et al. Electroluminescence from Colloidal Semiconductor CdSe Nanoplatelets in Hybrid Organic-Inorganic Light Emitting Diode. *Chem. Phys. Lett.* **2014**, *619*, 185−188.

(28) Rowland, C. E.; et al. Picosecond energy transfer and multiexciton transfer outpaces Auger recombination in binary CdSe nanoplatelet solids. *Nat. Mater.* **2015**, *14*, 484−489.

(29) Wood, V.; et al. Air-Stable Operation of Transparent, Colloidal Quantum Dot Based LEDs with a Unipolar Device Architecture. *Nano Lett.* **2010**, *10*, 24−29.

(30) Empedocles, S. a. Quantum-Confined Stark Effect in Single CdSe Nanocrystallite Quantum Dots. *Science.* **1997**, *278*, 2114−2117.

DOI: 10.1021/acs.nanolett.5b01233
Nano Lett. XXXX, XXX, XXX−XXX